CROATICA CHEMICA ACTA
CCACAA **77** (3) 469–476 (2004)
ISSN-0011-1643
CCA-2949
Original Scientific Paper

Precipitation and Characterization of Two Novel Aluminum Hydroxo Phthalates Formed in the Presence of Silicic Acid

László Horváth,[a,*] Halka Bilinski,[a] Lajos Radics,[b] and Nils Ingri[c]

[a]*Department of Physical Chemistry, Ruđer Bošković Institute, P.O. Box 180, HR-10002 Zagreb, Croatia*

[b]*Central Research Institute for Chemistry, Hungarian Academy of Sciences, Budapest, Hungary*

[c]*Department of Inorganic Chemistry, University of Umeå, Sweden*

RECEIVED NOVEMBER 7, 2003; REVISED FEBRUARY 19, 2004; ACCEPTED FEBRUARY 27, 2004

The present work, performed at constant ionic strength of 0.6 mol dm^{-3} NaCl at 25 °C, is a continuation of long-term studies of the conditions necessary for initial clay formation in model systems containing organic acids, Al and Si. Solid phases and the precipitation boundary characterizing the system H^+-Al^{3+}-phthalic acid (H_2L)-silicic acid were determined and compared with the previously found compound $Al_2(OH)_4L \cdot 4H_2O$ (A) of a monoclinic unit cell, which was formed in the absence of Si. Addition of Si induced precipitation of two novel compounds (B and C) of the orthorhombic unit cell. Compound B was formed at a low L/Al ratio ($R \leq 2$) and was of variable composition: $Al_x\,Si_{1.450-0.725x}\,(OH)_{3.8+0.1x}\,L \cdot 6H_2O$. It was found by calculation that at $R \leq 2$ the end member with $x = 2$, $Al_2(OH)_4L \cdot 6H_2O$, determined the precipitation boundary. Compound C formed at $R > 2$ had the constant composition $Al(OH)L \cdot 3H_2O$. Formation constants $\beta_{p,q,r}$ were determined for the general equation $pH^+ + qAl^{3+} + rL^{2-} \rightarrow H_pAl_qL_r$. The obtained values for compounds B and C are: $\log\beta(-4, 2, 1) = -7.40\pm0.10$ and $\log\beta\ (-1, 1, 1) = 1.55\pm0.05$, respectively. In addition to chemical analysis, thermogravimetry (TG), X-ray diffraction (XRD), infrared spectroscopy (IR), solid state ^{27}Al MAS NMR, ^{29}Si MAS NMR and ^{23}Na MAS NMR techniques were used for better characterization of solids and to detect possible impurities in them. Aluminum was found to be hexa-coordinated in all compounds. The IR spectra suggest that the phthalate ion acted as a bidendate ligand, bridging two aluminum atoms in solids B and C.

Key words
aluminum hydroxo phthalates
formation constants
effect of silicic acid
model clay formations
solid state NMR
^{27}Al MAS NMR
^{29}Si MAS NMR
^{23}Na MAS NMR

INTRODUCTION

The present work is a continuation of our long-term research program on precipitation reactions of Al and Fe with small organic ligands,[1–6] which are of special relevance to environmental chemists, geochemists, soil scientists and possibly neuroscientists. Many low molecular weight organic acids (LMWOA) have a high complex forming ability with Al^{3+}, and Fe^{3+}, and can act as the means of metal transport in soil profiles.[7] Besides the environmental interest in the phthalate ligand, there is a continuous interest in the hydrogen phthalate ion connected with the fundamental studies of hydrogen bonding.[8]

* Author to whom correspondence should be addressed. (E-mail: laszlo@irb.hr)

Complexation and precipitation reactions in the subsystem (without the presence of silicic acid) were studied[2] prior to the present work. In homogeneous solutions, two binary and three polynuclear mixed Al-hydroxo complexes were obtained. The possible binary complex AlL_3^{3-} was not detected[2] in the studied concentration range, low in Al (1–2 mmol dm^{-3}) and in excess of ligand. Comparable concentration of Al (10 mmol dm^{-3}) was titrated[2] at $R \leq 1$, where AlL_3^{3-} could not be expected. Only one phase $Al_2(OH)_4L \cdot 4H_2O$ of the monoclinic unit cell was found[2] to determine the precipitation boundary in the absence of silicic acid. The aim of the present study was to investigate the effect of silicic acid when added to the system and to characterize the formed novel phases, if any.

EXPERIMENTAL

Chemicals

$AlCl_3 \cdot 6H_2O$ (Merck) was dissolved in doubly distilled water. The Al(III) content of the stock solution was determined by indirect titration with EDTA-$Pb(NO_3)_2$, using the xylenol orange indicator;[9] $Na_2SiO_3 \cdot 9H_2O$ (Barker, *p.a.*) was dissolved in an acidic solution with H^+-excess. Determination of total silica was performed as described.[10] Sodium chloride, NaCl (Merck, *p.a.*) was dried at 180 °C and used without further purification to adjust the total ionic strength to 0.6 mol dm^{-3}. Sodium hydroxide solution was prepared from NaOH (Merck, *p.a.*) and standardized against acid. Phthalic acid (Merck, *p.a.*) was used without further purification after drying. It was dissolved either in doubly distilled water or in NaOH solution and its concentration was determined potentiometrically.

Instruments

A Zeiss tyndallometer combed with a Pulfrich photometer was used to detect the formation of solid phases. XRD diffractograms were taken with a Rigaku (Geigerflex/D/Max IIA) diffractometer using Cu-Kα radiation. TG analysis was carried out on a Cahn RG electroanalytical balance at a heating rate of 2 °C/min in air. The pH measurements were performed by a Radiometer 26 pH-meter, using a combined GK 2322 C electrode calibrated by Titrival buffer of pH = 5.00.

TABLE I. Experimental data for the precipitation boundary in the system H^+-Al^{3+}-phthalic acid-silicic acid in 0.6 mol dm^{-3} NaCl

$[Al]_T$ / mmol dm^{-3}	$[H_2L]_T$ / mmol dm^{-3}	$[Si]_T$ / mmol dm^{-3}	$-H_{min}$[(a)] / mmol dm^{-3}	pH_{min}	$-H_{max}$[(a)] / mmol dm^{-3}	pH_{max}	t / days
10	2	2	2.50	4.50	2.60	4.52	1
10	3.2	2	1.12	3.94	1.27	3.96	1
10	5	2	1.30	3.88	1.40	3.89	1
10	10	2	2.20	3.86	2.30	3.89	1
10	15	2	3.10	3.92	3.20	3.95	1
10	20	2	3.90	4.00	4.00	4.06	1
10	30	2	5.20	4.03	5.40	4.12	1
10	50	2	7.50	4.02	7.70	4.08	1
10	60	2	8.40	4.03	9.15	4.10	1
10	30	2	5.00	3.95	5.20	4.03	30
10	50	2	7.10	3.83	7.30	3.92	30
10	60	2	7.90	3.72	8.40	3.86	30
10	5	1	1.10	3.76	1.60	3.84	540
10	10	1	2.05	3.80	2.15	3.84	540
10	50	1	7.20	3.90	7.70	4.05	540
10	70	1	10.20	3.82	11.20	4.23	540
10	20	2	3.70	3.88	3.80	3.91	540
10	25	2	4.50	3.95	4.60	3.96	540
10	30	2	5.30	4.00	5.40	4.10	540
10	40	2	6.20	3.94	6.30	4.01	540
10	50	2	7.20	3.90	7.40	3.94	540
10	60	2	8.00	3.83	8.20	3.87	540
10	70	2	10.90	4.07	11.70	4.27	540
10	5	3	1.40	3.74	1.50	3.76	540
10	10	3	2.10	3.73	3.00	4.04	540
10	50	3	7.60	3.81	8.10	3.98	540
10	70	3	10.60	4.02	11.60	4.30	540
10	70	3				4.55	540
10	70	3	13.60	4.76	14.60	4.99	540

(a) The analytical proton deficit at the solubility boundary for the last clear and the first turbid point.

IR spectra were recorded on a Perkin-Elmer infrared spectrophotometer, Model 580 B, using KBr pellets.

Solid state NMR spectra were recorded at ambient temperature using a Varian Associates model Unity Inova spectrometer, operating at 79.44, 104.20 and 105.78 MHz, respectively, for ^{29}Si, ^{27}Al and ^{23}Na nuclei and a 7 mm broadband magic angle spinning (MAS) probe. Thick-wall zirconium rotors were filled with equal amounts of finely powdered samples and spun at an approximately 4.5 KHz spin rate and pulse sequence s2pu1. Spectra were recorded in the absolute value mode under identical experimental conditions.

Chemical shifts were referenced to external $Al_2(SO_4)_3 \cdot 18H_2O$ (0 ppm), NaCl (0 ppm) and tetrakis(trimethylsilyl)silane (–9.6 ppm).

The present investigation was carried out at 25.0 ± 0.1 °C at a constant ionic strength of 0.6 mol dm^{-3} (NaCl).

RESULTS AND DISCUSSION

Precipitation Data

Experimental data for determination of the precipitation boundary are presented in Table I. They have been collected for the amount ratio, R(Al, Si) = 10 : 2 and the ratio of phthalic acid to aluminum ranging from 0.2 to 7. Aging time was 24 h and 30 d. Other series of experiments were performed for R = 10 : 1, 10 : 2 and 10 : 3 with prolonged aging of 540 days. The method was first used by Težak *et al.*[11] and was later described in detail for similar systems to the one studied here.[1,12] The analytical proton deficit at the solubility boundary was calculated as earlier[12] for the last clear and the first turbid point as:

$$-H_{min} = NaOH_{min} + 2Na_2SiO_3$$

$$-H_{max} = NaOH_{max} + 2Na_2SiO_3$$

The value of pH_{min} in Table I indicates the corresponding pH value for the last clear point before precipitation, showing turbidity of doubly distilled water. The value of pH_{max} was measured in the first turbid point with a weak Tyndall effect as close as possible to the last clear point. A number of precipitates were isolated from the solution close to the precipitation boundary and were analyzed. At the ratio $R \leq 2$, the precipitated solid (B) was poorly crystalline and showed variable composition:

$Al_xSi_{1.450-0.725x}(OH)_{3.8+0.1x}L \cdot 6H_2O$, while at the ratio $R > 2$, the precipitated solid showed an almost constant composition $Al(OH)L \cdot 3H_2O$, with only traces of Si. Table II provides the X-ray diffraction data of solid B, prepared at $[Al]_T = [L]_T$ = 10 mmol dm^{-3}, $[Si]_T$ = 2 mmol dm^{-3} and pH = 4.13. (*Anal.* Found; mass fractions, w / %: Al, 11.54; C, 26.72; H, 4.91; Si, 2.02; L.O.I., 74.0). The rather poor X-ray pattern could be tentatively indexed with an orthorhombic unit cell of the dimensions a = 10.50 Å, b = 16.85 Å and c = 13.62 Å. The data are presented in the form of 2Θ, the corresponding $d_{obs.}$ and $d_{calc.}$ spacing and the relative intensities for the 6 highest peaks. With the molecular weight M_z = 375.07 and molecular volume V = 2409.7 Å^3, crystal density is given by the expression $D_{calc.} = 0.2585 \cdot Z$, where Z is the number of formula units in the unit cell. The value $D_{meas.}$ = 1.53 in paraffin oil can be explained if Z = 6 ($D_{calc.}$= 1.55).

TABLE II. X-ray powder diffraction data of $Al_xSi_{1.450-0.725x}(OH)_{3.8+0.1x}$ phthalate · 6 H_2O

2Θ / deg	d_{obs} / Å	d_{calc} / Å	h	k	l	I / I_o
5.240	16.849	16.849	0	1	0	39
6.482	13.621	13.620	0	0	1	100
8.423	10.495	10.500	1	0	0	34
16.717	5.300	5.296	0	2	2	34
25.330	3.514	3.500	3	0	0	25
28.530	3.126	3.123	1	5	1	26

Table III contains the X-ray powder diffraction data of the fairly crystalline solid C. This solid was prepared at $[Al]_T$ = 10 mmol dm^{-3}, $[L]_T$ = 60 mmol dm^{-3}, and $[Si]_T$ = 2 mmol dm^{-3}, at pH = 4.20. (*Anal.* Found w/%: Al, 12.10; C, 36.44; H, 3.97; Si, 1.30; Na, 0.70; L.O.I., 73.6). The 26 peaks could be indexed with an orthorhombic unit cell of the dimensions a = 12.67 Å, b = 15.66 Å and c = 14.17 Å.

With the molecular weight M_z = 261.96 and molecular volume V = 2810.2 Å^3 the crystal density is given by the expression $D_{calc.}$= 0.1548 Z, where Z is the number of formula units in the unit cell. The value $D_{meas.}$ = 2.06 in paraffin oil can be explained if we assume Z = 13 ($D_{calc.}$= 2.01). Sample C studied by XRD contained 0.12 SiO_2/Al and this would increase the molecular weight to M_z = 269.28, which gives the calculated density:

$$D_{calc.} = 2.068.$$

IR Spectral Characteristics

Figure 1 represents a part of IR spectra from 1900 to 200 cm^{-1} of solid B (spectrum a) and of solid C (spectrum b) while the IR spectrum of reference solid A was published earlier.[2] Only the most characteristic features of the IR spectra will be discussed, using the conventions of Nakamoto[13] and others.[14,5] A broad absorption band (not shown here) with the minimum at 3400 cm^{-1} originates from the O–H stretching of water molecules and OH^- groups. The broadness of this band indicates the presence of hydrogen bonding. A similar broad band was found earlier for solid A (see Figure 2, Ref. 2). The weak shoulder at 1710 cm^{-1} assigned[5] to carboxyl ν(C=O) exists in phases C and B, while it was not observed in phase A. A similar weak band was found[5] in numerous iron phtha-

TABLE III. X-ray powder diffraction data of the phase C, Al(OH)phthalate · $3H_2O$

2Θ / deg	d_{obs} / Å	d_{calc} / Å	h	k	l	I / I_o
5.631	15.687	15.661	0	1	0	8
6.280	14.061	14.166	0	0	1	100
6.974	12.664	12.667	1	0	0	20
9.533	9.266	9.443	1	0	1	3
10.922	8.092	8.086	1	1	1	3
11.339	7.792	7.831	0	2	0	5
12.330	7.170	7.083	0	0	2	4
14.435	6.131	6.182	1	0	2	5
15.189	5.828	5.871	2	1	0	6
16.397	5.405	5.424	2	1	1	7
17.837	4.969	4.924	2	2	0	8
18.262	4.855	4.852	1	2	2	11
18.676	4.749	4.722	0	0	3	5
19.479	4.554	4.569	1	3	1	5
21.160	4.195	4.202	0	3	2	5
22.373	3.969	3.988	1	3	2	4
22.669	3.919	3.918	3	1	1	7
22.988	3.865	3.875	2	3	1	5
25.049	3.551	3.542	0	0	4	4
25.442	3.488	3.502	2	3	2	6
25.806	3.449	3.454	0	1	4	5
26.104	3.410	3.411	1	0	4	5
27.812	3.205	3.198	3	3	1	4
28.207	3.162	3.167	4	0	0	5
28.971	3.080	3.086	3	1	3	6
29.412	3.034	3.033	2	1	4	4

lates precipitated at low pH. The band at 1570 cm^{-1} was assigned to the asymmetric stretching frequency of coordinated COO^- groups. This band is split and is significantly broader than in solid A. The strong composite band at 1425 cm^{-1} assigned to ν_{sym} (COO^-) contains two side bands at 1450 cm^{-1} and at 1395 cm^{-1} of different intensities. The OH^- deformation vibration of the carboxyl group found at 910 cm^{-1} in phthalic acid was not recorded in any of the three solids (A, B and C). It was shifted to 965 cm^{-1} in solid A. Overlapping with Si–O vibrations, originating from possible impurities, was found in this region but the nature of such silicate impurity could not be detected by the IR method. The band at 750 cm^{-1} can be assigned to Π(C–C), and bands at 700 cm^{-1} and 650 cm^{-1} to $\delta(COO^-)$ + Π(COO^- or OH^-). There is a difference in the region belonging to the Al–OH stretches. A broad unresolved band was found in solid B. A rather strong and resolved band was found in solid C. A strong split band was found in solid A. The separation Δ145 cm^{-1} in

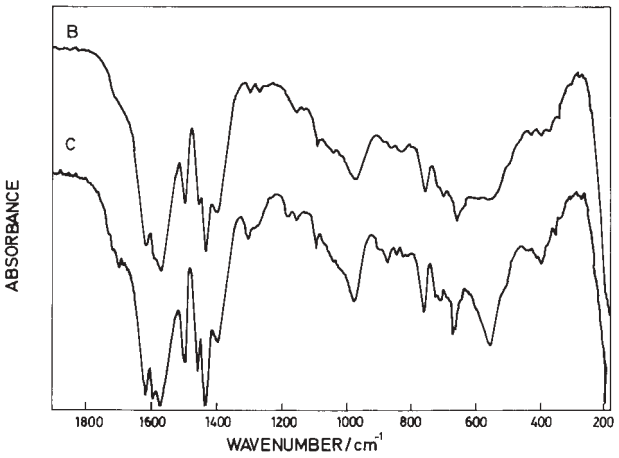

Figure 1. IR spectrum of Al_x $Si_{1.450-0.725x}$ $(OH)_{3.8+0.1x}$ L · 6 H_2O for $x = 2$ (compound B) precipitated at $[L]_T / [Al]_T < 2$; IR spectrum of AL(OH)L · $3H_2O$ (compound C), precipitated at $[L]_T / [Al]_T > 2$. Concentration of $[Al]_T$ = 10 mmol dm^{-3}, $[Si]_T$ = 2 mM, pH ≈ 4.2 and 0.6 mol dm^{-3} NaCl.

solids B and C of the composite ν_{as} and ν_{sym} frequencies is smaller than that in the free phthalic acid (Δ281 cm^{-1}), but greater than 120 cm^{-1} found earlier[2] in solid A. It suggests that the phthalate ion acts as a bidendate ligand, bridging two aluminum ions in solids B and C, similarly as found for zirconium hydroxo phthalate.[14] According to Nakamoto,[13] this separation should be about Δ100 cm^{-1} for the carboxyl group acting as a bidendate ligand toward the same metal atom.

Until now, our numerous attempts have failed to prepare single crystals of adequate quality to verify the structural features; therefore the IR evidence should be regarded as tentative.

Solid State NMR Spectra

As reviewed by S. Frančišković,[15] different NMR techniques are currently used in soil and sediment characterization as complementary to other analytical methods. The usage of solid state NMR spectroscopy is particularly advantageous because it does not depend on the solubility of samples.[16] In the present work, NMR spectra were used as a complementary method to demonstrate the differences in precipitated compounds.

^{27}Al MAS NMR spectra were used to obtain information about co-ordination of Al atoms. ^{29}Si MAS NMR and ^{23}Na MAS NMR spectra were also used to detect the kind of possible Si or Na containing impurities in the studied samples.

^{27}Al MAS NMR spectra of compounds A, B, C, with numbers for chemical shifts, are represented in Figure 2 (a–c). They show broad multi-component aluminium-27 spectra centered from – 0.85 to – 10.61 ppm, characteristic of the non-framework hexa-coordinated octahedral Al atoms. Deconvolution of the spectra revealed that the individual components, including spinning side-bands, ex-

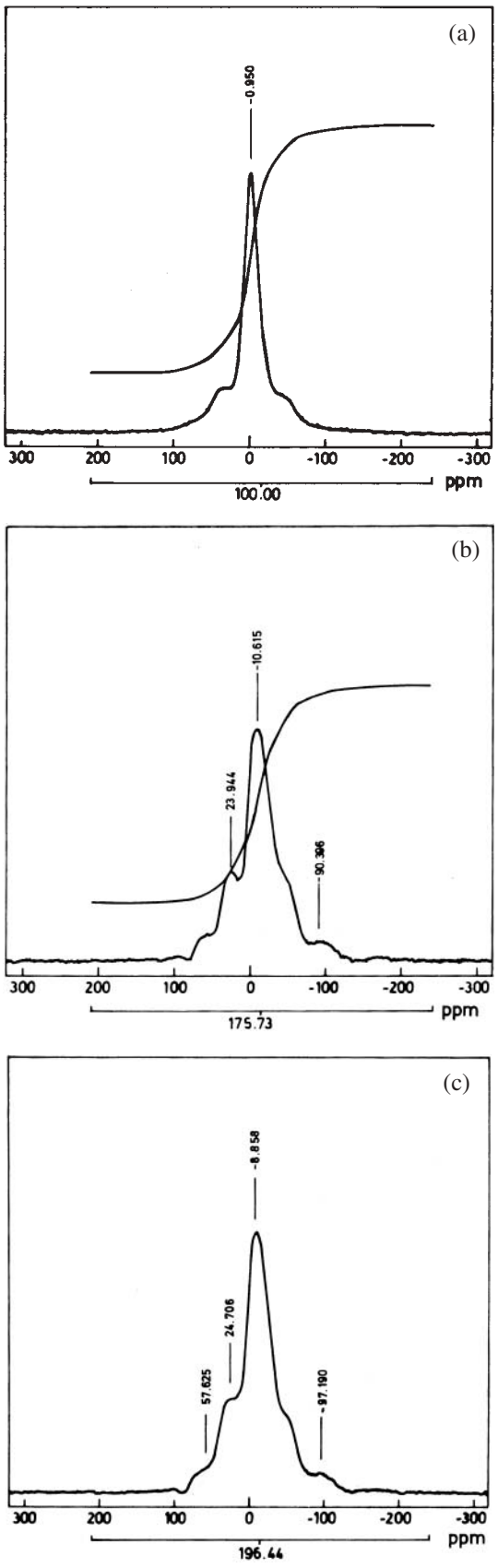

Figure 2. 104.2 MHz ^{27}Al MAS NMR spectra: a) Reference compound $Al_2(OH)_4L \cdot 4H_2O$, (compound A) precipitated in the absence of Si and studied earlier;[2] b) compound $Al_2(OH)_4L \cdot 6H_2O$; c) compound $Al(OH)L \cdot 3H_2O$.

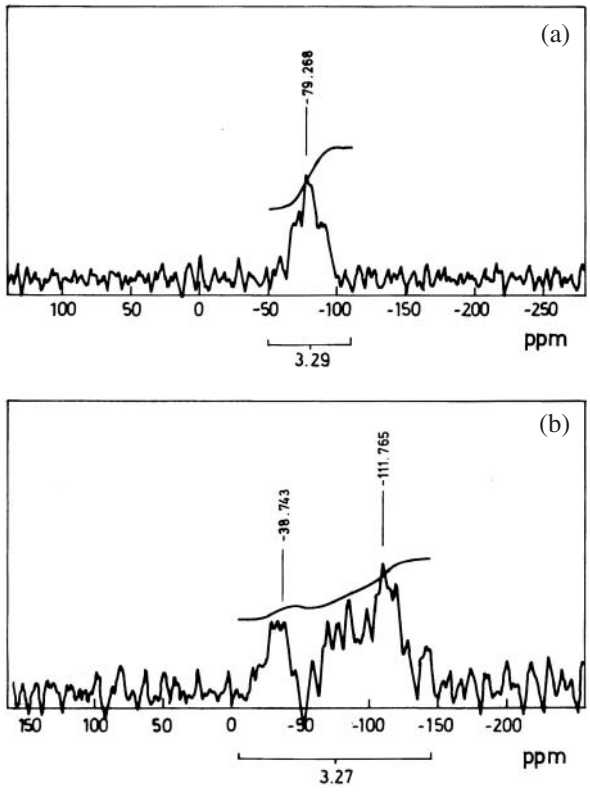

Figure 3. 79.5 MHz ^{29}Si MAS NMR spectra indicating silicate impurities in: a) compound $Al_2(OH)_4L \cdot 6H_2O$, b) compound $Al(OH)L \cdot 3H_2O$.

tend over the 100–150 ppm range and most likely reflect the varying quadrupolar interactions of Al nuclei with the surrounding heterogeneous lattice. Highly inhomogeneous local environments can be suggested. Contrary to these results, two aluminum silicates measured under identical conditions showed narrow resonances (~10 ppm), which will be published elsewhere. For details of the ^{27}Al MAS NMR technique applied on clays the reader is referred to the review paper of Akitt.[17]

^{23}Na MAS NMR spectra showed a very weak singlet (line width: 5 ppm) at –11.627 ppm, practically identical for each sample and carrying no structural information whatsoever. These are related to NaCl impurities, because samples were prepared from 0.6 M NaCl solutions.

^{29}Si MAS NMR spectra of compounds B and C are shown in Figure 3 (a, b). Signals are broad and have different shapes. For sample B, the spectrum shows a resonance typical of Al-silicates with a high Al-content. The Si spectrum of sample C with two broad peaks covering the range between –20 to –130 ppm does not resemble Al-silicates and is hard to understand. A reference spectrum of H_4SiO_4 shows no similarity with the broad peak centered at –117.700 ppm. According to Watanabe *et al.*,[18] it would be unwise to attempt determining the structures from chemical shifts, especially for poorly crystalline solids. For details on ^{29}Si MAS NMR, the reader is referred to the review of Engelhardt and Michael.[19]

TABLE IV. Composition matrix of binary and ternary complexes and solid phases in the system H^+-Al^{3+}-H_2L-H_2SiO_4 in 0.6 mol dm^{-3} NaCl [a]

	Tentative structure	log β	p	q	r	t	u	Phase	Ref.
1	H	0	1	0	0	0	0	Soluble	
2	Al	0	0	1	0	0	0	Soluble	
3	L	0	0	0	1	0	0	Soluble	
4	Si	0	0	0	0	1	0	Soluble	
5	Na	0	0	0	0	0	1	Soluble	
6	HL	4.649	1	0	1	0	0	Soluble	2
7	H_2L	7.275	2	0	1	0	0	Soluble	2
8	AlL	2.94	0	1	1	0	0	Soluble	2
9	AlL_2	4.97	0	1	2	0	0	Soluble	2
10	AlL_3	7.10	0	1	3	0	0	Soluble	This work
11	AlOH	–5.52	–1	1	0	0	0	Soluble	21
12	$Al(OH)_2$	–10.30	–2	1	0	0	0	Soluble	22
13	$Al(OH)_3$	–16.17	–3	1	0	0	0	Soluble	22
14	$Al(OH)_4$	–23.46	–4	1	0	0	0	Soluble	23
15	$Al_3(OH)_4$	–13.57	–4	3	0	0	0	Soluble	21
16	$Al_{13}O_4(OH)_{24}$	–105.5	–32	13	0	0	0	Soluble	21
17	$Al_3(OH)_4L$	–8.47	–4	3	1	0	0	Soluble	2
18	$Al_2(OH)_2L$	–2.50	–2	2	1	0	0	Soluble	2
19	$Al_2(OH)_2L_2$	–0.07	–2	2	2	0	0	Soluble	2
20	$Al(OH)_3$ (s)	–11.4	–3	1	0	0	0	Solid	24
21	$Al_2(OH)_4L \cdot 6H_2O$ (s)	–7.40	–4	2	1	0	0	Solid	This work
22	Al(OH)L (s)	1.55	–1	1	1	0	0	Solid	This work
23	$Al(OH)_3H_4SiO_4$	–8.00	–3	1	0	1	0	Solid	12
24	$Al_2(OH)_6H_4SiO_4$	–18.60	–6	2	0	1	0	Solid	12
25	$NaAl(OH)_4H_4SiO_4$	–13.20	–4	1	0	1	1	Solid	12

[a] H_2L = phthalic acid.

Computer Calculations

Calculations of the model predominance area diagrams were performed using the SOLGASWATER program.[20] Equilibrium constants used in the model are summarized in Table IV. The model includes several constants that were determined earlier.[2,12,21–24] This table also includes the till now unknown formation constants $\beta(-4,2,1)$ and $\beta(-1,1,1)$ for solids B and C, which had to be adjusted to have constant values using data from Table I. For solid C, the formation constant was constant for each ligand concentration where C precipitated. It was a problem to explain which value of x gave a constant formation constant of solid B. After trying all possible values of x between 1.5 and 2, the constant value was obtained only for the end member with $x = 2$, $Al_2(OH)_4L \cdot 6H_2O$ of orthorhombic unit cell, which determines the shape of the solubility curve at $R \leq 2$. This value is different from the formation constant of reference compound A, $(Al_2(OH)_4L \cdot 4H_2O$, of a monoclinic unit cell),[2] which did not precipitate at the solubility boundary in the presence of Si. Although phase B has an identical ratio of $[Al]_T / [L]_T$, it has more crystal water and is different from phase A from the structural point of view.

To explain the increased dissolution of $Al(OH)L \cdot 3H_2O$ (observed at Al = 10 mmol dm^{-3}; L = 70 mmol dm^{-3}; Si = 3 mmol dm^{-3}, pH = 4.7 after aging 540 days), an additional soluble complex AlL_3 was added in Table IV to the model. This complex was not detected earlier[2] in homogeneous solutions in excess of the ligand and at ten times lower concentrations of total Al. Potentiometric titration[2] could not be used at the high concentrations used in this work. The silicate complex of Al in acid solution (pH < 4) was reported to be negligible[25] and is not included in the model. The predominance area diagram presented in Figure 4 was calculated using the speciation scheme given in Table IV, showing the stability areas of solids B and C and predominant species in solution. Com-

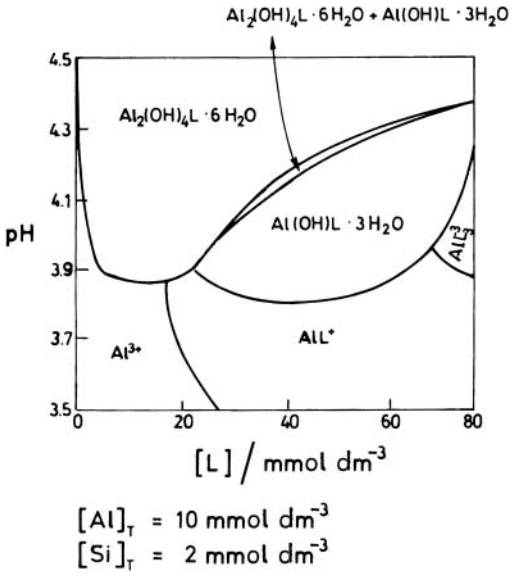

Figure 4. Predominance area diagram pH *vs.* $[L]_T$ / mmol dm^{-3}, calculated for $[Al]_T$ = 10 mmol dm^{-3}, $[Si]_T$ = 2 mmol dm^{-3}. It represents the area of stable solid compounds B and C in equilibrium with the predominating Al species in solution.

paring the predominance area diagram in the absence of Si (Figure 6, Ref. 2), it can be observed that in the presently studied system Si induced precipitation of two binuclear aluminum hydroxo phthalates, otherwise soluble in the absence of Si, from which complex $Al_2(OH)_2L^{2+}$ is further hydrolyzed. The Al^{3+} ion and AlL^+ complex predominated in solution, as it was also found in the absence of Si, but precipitation started at lower pH values. Complex AlL_3^{3-} was necessary to explain the increased solubility in high excess of the ligand.

CONCLUSIONS

(i) When added to the H^+-Al^{3+}-phthalic acid-NaCl (0.6 mol dm^{-3}) system, silicic acid induced precipitation of two novel aluminum hydroxo phthalates. At the ratio $[L]_T$ / $[Al]_T$ < 2, the precipitated solid showed variable composition: $Al_xSi_{1.450-0.725x}(OH)_{3.8+0.1x}L \cdot 6H_2O$, with x = 1.5–2.0. The end member with x = 2 ($Al_2(OH)_4L \cdot 6H_2O$) of orthorhombic unit cell determines a part of the precipitation boundary (sample B).

At the ratio $[L]_T$ / $[Al]_T$ > 2, the precipitated solid showed good crystallinity with a practically constant composition: $Al(OH)L \cdot 3H_2O$. This phase (sample C) determines the precipitation boundary in excess of the ligand. Both solids contain traces of silicate.

(ii) ^{27}Al MAS NMR spectra of reference sample (A) of a monoclinic unit cell, $Al_2(OH)_4L \cdot 4H_2O$, and of two new compounds (samples B and C) are broad multi-component spectra, centered from –0.95 to –10.61 ppm, characteristic of non-framework, hexa-coordinated octahedral Al.

(iii) ^{29}Si MAS NMR spectra are not pronounced, suggesting the presence of impurities. In sample B, the spectrum resembles the spectra of Al-silicate. Spectrum C could not be interpreted.

(iv) Formation constants of two novel aluminum hydroxo phthalates (B and C) were calculated: $\beta(-4,2,1)$ = –7.40±0.10 and $\beta(-1,1,1)$ = 1.55±0.05. »Errors« represent 3τ. An additional soluble complex AlL with $\beta(0,1,3)$ = 7.10±0,20 was added to the model to explain dissolution in excess of the ligand (70 mmol dm^{-3}) at a high Al concentration (10 mmol dm^{-3}). It is rather unusual that K_3 is greater than K_2 and the reason is not yet known. It was assumed that the previous[2] solution model was correct under the studied conditions, but not completed due to the limitations of potentiometric titration. Therefore, the formation constant of AlL_2 from Ref. 2 was not varied in the calculation, only AlL_3 was adjusted.

Silicate complexes of Al in acid solution at pH < 4 were negligible[25] and therefore not considered in the applied model from Table IV. None of the Al-silicates were formed under low pH values at the solubility boundary.

(v) Similarly as found earlier for aluminum with oxalate ligand,[1] aluminum hydroxo phthalates could be considered as metastable phases in the hydrolytic transformation of the aqueous aluminum complexes down to stable aluminum hydroxide.

Acknowledgements. – The present research was performed within the project No. 0098041 of the Ministry of Science and Technology, Croatia. It was partly supported by the Swedish National Science Research Council and USGS-Croatia project (JF-169). We thank Prof. Staffan Sjöberg for his fruitful discussions during the work and for correction of the first prepared manuscript. Thanks are also due to the two anonymous reviewers of CCA who have largely contributed to the improvement of the manuscript.

REFERENCES

1. H. Bilinski, L. Horvath, N. Ingri, and S. Sjöberg, *Geochim. Cosmochim. Acta* **50** (1986) 1911–1922.
2. T. Hedlund, H. Bilinski, L. Horvath, N. Ingri, and S. Sjöberg, *Inorg. Chem.* **27** (1988) 1370–1374.
3. Darko Hanžel, D. Hanžel, H. Bilinski, T. A. Himdan, M. Miljak, and V. Vančina, *Hyperfine Interact.* **53** (1990) 339–344.
4. M. Tonković, H. Bilinski, and M. E. Smith, *Inorg. Chim. Acta* **197** (1992) 59–65.
5. V. Vančina, T. A. Himdan, H. Bilinski, M. Miljak, I. Kos, D. Hanžel and Darko Hanžel, *Thermochim. Acta* **229** (1994) 199–212.
6. M. Tonković and H. Bilinski, *Polyhedron* **14** (1995) 1025–1030.
7. P. A. W. van Hees, A.-M. T. van Hees, and U. S. Lundstrõm, *Soil Biol. Biochem.* **33** (2001) 867–874.
8. J. S. Loring, M. Karlsson, W. R. Fawcett, and W. H. Casey, *Spectrochim. Acta* **A57** (2001) 1635–1642.

9. L.-O. Öhman and S. Sjöberg, *Acta Chem. Scand., Ser. A* **35** (1981) 201–212.
10. S. Sjöberg, A. Nordin, and N. Ingri, *Mar. Chem.* **10** (1981) 521–532.
11. B. Težak, E. Matijević, and K. Schulz, *J. Am. Chem. Soc.* **73** (1951) 1602–1605.
12. H. Bilinski, L. Horvath, N. Ingri, and S. Sjöberg, *J. Soil. Sci.* **41** (1990) 119–132.
13. K. Nakamoto, *Infrared and Raman Spectra of Inorganic and Coordination Compounds,* 3rd ed., Wiley, New York, 1978.
14. H. Bilinski, N. Brničević, and Z. Konrad, *Inorg. Chem.* **20** (1981) 1882–1885.
15. S. Frančišković, Application of NMR technique in sediment and soil characterization, *Book of Abstracts,* DU 2003 NMR, (The 4th International Dubrovnik NMR Course and Conference, June 28 – July 01, 2003, Dubrovnik) p. 7.
16. M. W. I. Schmidt, H. Knicker, P. G. Hatcher, and I. Kögel-Knaber, *J. Sci.* **48** (1997) 319–328.
17. J. W. Akitt, *Prog. Nucl. Magn. Res. Spectrosc.* **21** (1989) 1–149.
18. T. Watanabe, H. Shimizu, K. Nagasawa, A. Masuda, and H. Saito, *Clay Miner.* **22** (1987) 37.
19. G. Engelhardt and D. Michel: *High-Resolution Solid-State NMR of Silicates and Zeolites*, John Wiley&Sons, Chichester, 1986.
20. G. Eriksson, *Anal. Chim. Acta* **112** (1979) 375–383.
21. L.-O. Öhman and W. Forsling, *Acta Chem. Scand., Ser. A* **35** (1981) 795–802.
22. C. F. Baes and R. E. Mesmer: *The Hydrolysis of Cations*. Wiley, New York, 1976, p. 121.
23. L.-O. Öhman, S. Sjöberg, and N. Ingri, *Acta Chem. Scand., Ser. A* **37** (1983) 561–568.
24. N. Deželić, H. Bilinski, and R. H. H. Wolf, *J. Inorg. Nucl. Chem.* **33** (1971) 791–798.
25. T. W. Swaddle, *Coord. Chem. Rev.*, **219–221** (2001) 665–686.

SAŽETAK

Taloženje i karakterizacija dva nova spoja aluminijevoga hidroksoftalata nastaloga u prisustvu silikatne kiseline

László Horváth, Halka Bilinski, Lajos Radics i Nils Ingri

Ovaj rad izveden je uz konstantnu ionsku jakost od 0.6 mol dm^{-3} NaCl na 25 °C i predstavlja nastavak višegodišnjih istraživanja uvjeta potrebnih za stvaranje glina u modelnom sustavu koji sadržava organske kiseline, Al i Si. Kruta faza i taložna granica koje karakteriziraju sustav H^+-Al^{3+}-ftalna kiselina (H_2L)-silikatna kiselina određene su i uspoređene s ranije nađenim spojem $Al_2(OH)_4L \cdot 4H_2O$ (A) monoklinske jedinične ćelije koji je stvoren bez prisustva Si. Dodatak Si uzrokuje taloženje dva nova spoja (B i C) ortorombske jedinične ćelije. Spoj B nastaje kod niskih omjera L/Al ($R \leq 2$) i on je promjenljivoga sastava: $Al_x\ Si_{1.450\text{-}0.725x}\ (OH)_{3.8+0.1x}\ L \cdot 6\ H_2O$. Izračunano je da kod $R \leq 2$ krajnji produkt sa $x = 2$, spoj $Al_2(OH)_4L \cdot 6H_2O$ određuje taložnu granicu. Spoj C stvoren kod $R > 2$ ima konstantni sastav $Al(OH)L \cdot 3H_2O$. Konstanta stvaranja $\beta_{p,q,r}$ određena je za općenitu jednadžbu $pH^+ + qAl^{3+} + rL^{2-} \rightarrow H_pAl_qL_r$. Dobivene vrijednosti za spojeve B i C su : $\log \beta(-4, 2, 1) = -7.40 \pm 0.10$ i $\log \beta(-1, 1, 1) = 1.55 \pm 0.05$. Za bolju karakterizaciju krutina i određivanje mogućih onečišćenja u njima, uz kemijsku analizu, rabljene su termogravimetrija (TG), metoda difrakcije rentgenskih zraka (XRD), infracrvena spektroskopija (IR), ^{27}Al MAS NMR, ^{29}Si MAS NMR i ^{23}Na MAS NMR. Nađeno je da je Al heksakoordiniran u svim spojevima. IR spektar sugerira da ftalatni ion djeluje kao bidendatni ligand koji premošćuje dva Al atoma u spojevima B i C.